

A Two Dimensional Simulation of Crack Propagation using Adaptive Finite Element Analysis

Abdulnaser M. Alshoaibi*

Department of Mechanical Engineering, Jazan University, P. O. Box 706, Jazan 45142, Kingdom of Saudi Arabia

ARTICLE INFO

Article history:

Received: 30 August 2018

Accepted: 17 October 2018

Keywords:

Finite Element

Linear Elastic Fracture mechanics

Mesh Density

Stress Intensity Factor

ABSTRACT

Finite element method (FEM) is one of the most famous methods which has many applications in various studies such as the study of crack propagation in engineering structures. However, unless extremely fine meshes are employed, problem arises in accurately modelling the singular stress field in the singular element area around the crack tip. In the present study, the crack growth simulation has been numerically simulated by using the dense mesh finite element source code program using Visual FORTRAN language. This code includes the mesh generator based on the advancing front method as well as all the pre and post process for the crack growth simulation under linear elastic fracture mechanics theory. The stress state at a crack tip has been described by the stress intensity factor which is related to the rate of crack growth. The displacement extrapolation technique is employed to obtain crack tip singular stresses and the stress intensity factors values. The crack direction is predicted using the maximum circumferential theory. Verification of the predicted stress intensity factors and crack path direction are validated with relevant experimental data and numerical results obtained by other researchers with good agreements.

1. Introduction

The use of mesh generation methods for dividing a complex problem into small elements plays a crucial role in the finite element simulation, which determines the accuracy of the finite element model and the required computational time. The effectiveness of the mesh size distribution on the accurateness of numerical analysis results has been inspected by many researchers. Based on the finite element methods, as the mesh is fine with a small size as the precision of the results will be high but may take longer computational time. Furthermore, the simulation with coarse mesh leads to reduce the precision of the results with less computational time.

One of the most popular methods used to generate unstructured meshes is the advancing front method, first proposed by [1], with the more details form described by [2] and [3]. Most of the mesh generators utilizing advancing front techniques have been developed in the past few decades. The advancing front approach is known to be robust, versatile over domains of different dimensions with diverse geometrical and topological characteristics, and is able to generate elements of various types such as triangles, quadrilaterals, tetrahedra and hexahedra close to the well-shaped ideal geometry in compliance with the specified

node spacing specification. Lo [4] presented a dynamic grid approach for the advancing front method to generate adaptive triangular meshes of variable element size over arbitrary planar domains. He [4] proposed a simple domain partition scheme with little demand on additional memory, which could drastically reduce the search time over the generation front.

Malekan et al. [5] presented an object-oriented implementation of the extended finite element method to model the crack nucleation and propagation in structures made of either linear or nonlinear materials. They used the Stress intensity factor and singularity of the localization tensor to determine the crack propagation direction for linear elastic materials and nonlinear material models. Liu [6] obtained a methodical study on finding the effects of the mesh size on the accuracy of the finite element analysis results, based on which brief procedures of choosing best element size in finite element modeling are provided. Benamara et al. [7] proposed the displacement extrapolation technique (DET) for homogeneous materials to obtain the stress intensity factors (SIFs) at crack-tip. Soman et al. [8] proposed a simple and efficient finite element based technique using the crack face nodal displacements for the accurate estimation of mode I, mode II and mixed mode I/II stress intensity factors. Yaylaci [9] presented a comparative study of finite element method (FEM) and analytical method for the plane problem of a layered composite containing

* Corresponding author. Tel.: +966563479523; fax: +966 7 3232900 ; e-mail: alshoaibi@gmail.com

an internal perpendicular crack by using a finite element software ANSYS for two dimensional analysis. Main goal of the numerical simulation is to investigate the normal stress, stress intensity factors at the crack tip and the crack opening displacements.

An analytical-computational method along with finite element analysis (FEA) has been employed by [10] to analyze the dynamic behavior of deteriorated structures excited by time- varying mass. They focused on the comparative study of a double cracked beam with inclined edge cracks and transverse open cracks subjected to traversing mass. They also considered the influence of the parameters like crack depth and crack inclination angles are investigated on the dynamic behavior of the structure. More and Bindu [11] Studied, the effects of element size on the accuracy of finite element models has been studied by . They investigated that, through static analysis, and buckling analysis it was found that for static analysis which assumes steady loading and response conditions the model should be discretized into elements of size 40 mm in order to obtain accurate results, consuming fewer computer resources and computing time. For bucking analysis the FE model which is meshed between 30 and 50 mm size can give us an optimal combination of accuracy and efficiency.

The present software has been developed by using Visual FORTRAN language to enable the user to determine the fracture mechanics parameters such as the stress intensity factors history, the stress distribution, the strain distribution at each node and element, the deformed mesh, the crack path direction as well as the contour distribution.

2. Adaptive Mesh Refinement

Conceptually, the advancing front method is one of the simplest mesh generation processes. The element generation algorithm, starting from an initial ‘front’ formed from the specified boundary of the domain, generates element, one by one, as the front advances into the region to be discretized until the whole domain is completely covered by elements. The mesh is constructed by progressively adding mesh elements starting at the boundaries. This iteration results in a propagation of a front which is the border (internal boundary) between the meshed and the unmeshed region. The positions of the internal nodes are dependent on the element densities at these positions. The nodes on the front is updated, with the new element edges forming the new front. This process is continued, working into the interior of the domain until the whole of the object domain has meshed.

The mesh refinement can be controlled by the characteristic size of each element, predicted according to the error estimator. This initial mesh is modelled by the incremental theory adopting the von Mises yield criterion to solve the first model. At the end of each load step, the solution has converged in order to estimate the percentage of error based on the mesh size of each element. In the case of exceeding the specified maximum error at any point in the domain, the construction analysis is interrupted and a new mesh domain model is constructed ([12] and [13]). The element error estimator is subsequently used to compute the optimal mesh size as:

$$h_e = \sqrt{2A_e} \tag{1}$$

where A_e is the area of the triangle element. The norm stress error for each element is defined as:

$$\begin{aligned} \|e\|_e^2 &= \int_{\Omega^e} (\boldsymbol{\sigma} - \boldsymbol{\sigma}^*)^T (\boldsymbol{\sigma} - \boldsymbol{\sigma}^*) d\Omega \\ &= \int_{\Omega^e} \left(\begin{matrix} \sigma_x \\ \sigma_y \\ \tau_{xy} \\ \sigma_z \end{matrix} \right) - \left(\begin{matrix} \sigma_x^* \\ \sigma_y^* \\ \tau_{xy}^* \\ \sigma_z^* \end{matrix} \right)^T \left(\begin{matrix} \sigma_x \\ \sigma_y \\ \tau_{xy} \\ \sigma_z \end{matrix} \right) - \left(\begin{matrix} \sigma_x^* \\ \sigma_y^* \\ \tau_{xy}^* \\ \sigma_z^* \end{matrix} \right) d\Omega \end{aligned} \tag{2}$$

while the average norm stress error for the whole domain is

$$\|\hat{e}\|^2 = \frac{1}{m} \sum_{e=1}^m \int_{\Omega^e} \boldsymbol{\sigma}^T \boldsymbol{\sigma} d\Omega \tag{3}$$

where m is the number of total elements in the whole domain, $\boldsymbol{\sigma}$ and $\boldsymbol{\sigma}^*$ is the stress and smoothed stress vector respectively which components are clearly given in equation (2).

In the present study, we have attempted here to keep the error to 5% in the relative energy norm ζ_e less than some specified value ζ . Thus

$$\zeta_e = \frac{\|e\|_e}{\|\hat{e}\|} \leq \zeta \tag{4}$$

and the new element relative stress error norm with the permissible error of ζ defined as

$$\varepsilon_e = \frac{\|e\|_e}{\zeta \|\hat{e}\|} \leq 1. \tag{5}$$

This means any element with the new element size $\varepsilon_e > 1$ need to be refined and consequently, the new size of mesh refinement need to be constructed based on the new element size. Based on the new element size the asymptotic convergence rate criteria whereby is assumed as:

$$\|e\|_e \propto h_e^p \tag{6}$$

where p is the polynomial order of approximation. In our case $p = 2$ since we are using quadratic polynomial for the finite element approximation. The approximate size of the new element is:

$$h_N = \frac{1}{\sqrt{\varepsilon_e}} h_e \tag{7}$$

3. Determination of Stress Intensity Factors and Crack Direction

One of the most important parameters in linear elastic fracture mechanics is the stress intensity factor which is able to correlate the crack growth and fracture behavior. For this reason, the accurate value of the stress intensity factor must be predicted precisely in all steps of crack growth. In the present study, the displacement extrapolation method has been used to calculate the stress intensity factors values which depend on the nodal displacements around the crack tip. Crack tip elements based on this approach were proposed independently [14] and [15]. In this work, the natural triangle quarter point element is chosen as the crack tip elements type and their construction follows in the

schematic rosette formation around the crack tip as shown in Fig. 1. The near tip nodal displacements at nodes *b*, *c*, *d* and *e* shown in Fig. 1. The displacement tangential and normal to crack plane are denoted as *u'* and *v'* respectively.

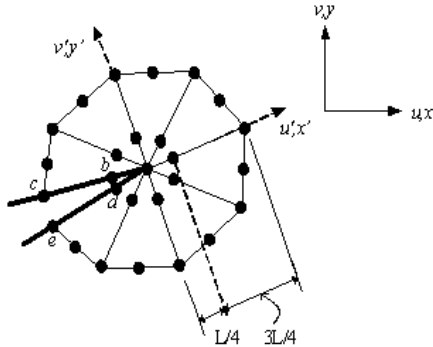


Fig. 1 The quarter-point singular elements around the crack tip.

The displacement extrapolation method configurations for estimation of mode I and mode II stress intensity factor are given by [16] as:

$$K_I = \frac{E}{(1+\nu)(1+\kappa)} \sqrt{\frac{2\pi}{L}} \left(2(v'_b - v'_d) - \frac{(v'_c - v'_e)}{2} \right) \quad (8)$$

$$K_{II} = \frac{E}{(1+\nu)(1+\kappa)} \sqrt{\frac{2\pi}{L}} \left(2(u'_b - u'_d) - \frac{(u'_c - u'_e)}{2} \right) \quad (9)$$

In order to simulate crack propagation under a linear elastic condition, the crack path direction must be determined. The maximum circumferential stress theory [17] asserts that, for isotropic materials under mixed-mode loading, the crack will propagate in a direction normal to maximum tangential tensile stress. In polar coordinates, the tangential stress is given by

$$\sigma_\theta = \frac{1}{\sqrt{2\pi r}} \cos \frac{\theta}{2} \left[K_I \cos^2 \frac{\theta}{2} - \frac{3}{2} K_{II} \sin \theta \right] \quad (10)$$

The direction normal to the maximum tangential stress can be obtained by solving $d\sigma_\theta/d\theta = 0$ for θ . The nontrivial solution is given by

$$K_I \sin \theta + K_{II} (3 \cos \theta - 1) = 0 \quad (11)$$

which can be solved as:

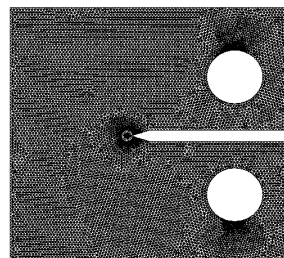
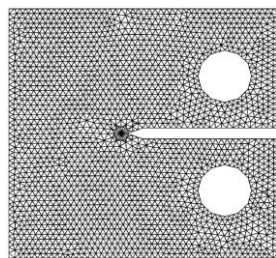


Fig. 3 Two different steps of the adaptive mesh for compact tension specimen

$$\theta = \pm \cos^{-1} \left\{ \frac{3K_{II}^2 + K_I \sqrt{K_I^2 + 8K_{II}^2}}{K_I^2 + 9K_{II}^2} \right\} \quad (12)$$

4. Results and Discussions

4.1 Compact Tension Specimen

Consider the geometry of a compact tension specimen with an initial crack length, $a = 9\text{ cm}$ and width, $W = 18.8\text{ cm}$ as shown in Fig. 2. The formula of stress intensity factor for this geometry according to ASTM Standard E-399-72 specimen can be obtained from [18] as follows:

$$K_I = P \left(2 + \frac{a}{W} \right) \left(0.886 + 4.64 \left(\frac{a}{W} \right) - 13.32 \left(\frac{a}{W} \right)^2 + 14.72 \left(\frac{a}{W} \right)^3 - 5.6 \left(\frac{a}{W} \right)^4 \right) / B \sqrt{W} \left(1 - \frac{a}{W} \right)^{3/2} \quad (13)$$

where P is the applied load and B is the specimen thickness.

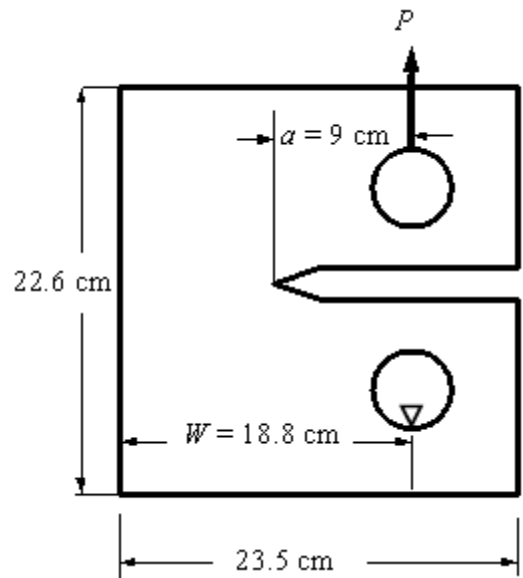


Fig. 2 Problem statements for the compact tension specimen

Fig. 3 shows two types of the generated mesh with different densities, however, as the mesh density is increased a high-quality contour plot is obtained as well as increasing the precision of the stress intensity factor prediction. The adaptively of the mesh density is clear which are needed at the vicinity of loading, fixity and near to the crack tip.

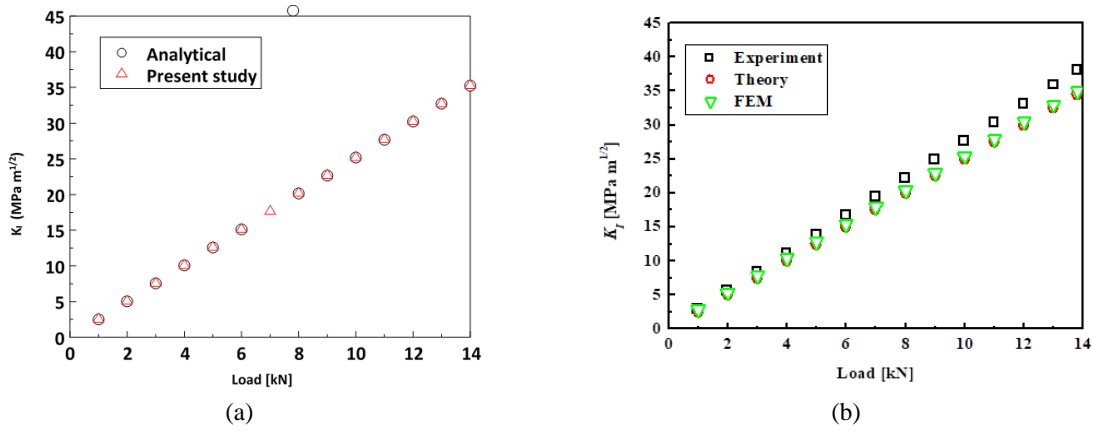


Fig. 4 Comparison of stress intensity factor, K_I values for steel specimen of thickness $B = 0.83$ cm with results from (a) the analytical formula and (b) [19]

The stress intensity factor K_I is calculated for a range of loads is compared with those of the analytical formula obtained in equation (13) as shown in Fig. (4a) and also the results of [19] as shown in Fig. 4b. Fig. 4 Comparison of stress intensity factor, K_I values for Steel specimen of thickness $B = 0.83$ cm with results from (a) the analytical formula and (b) [19] also include the analytical solution (labelled as ‘Theory’ in the legend) and ANSYS FEM solution beside their experimental result. The analytical formula correlates very well with the numerical result under the plane stress condition.

Fig. 5 shows the calculated stress intensity factor for the Aluminium specimen compared to the analytical solution. The relative error is very small for all values. Since the difference is very small, one can conclude that the material properties do not have an effect on the stress intensity factors values under linear elastic assumption. The numerical result for steel specimen is more accurate than that for Aluminium with reference to the analytical formula.

Fig. 6(a) shows the normal principal stress σ_1 and Fig. 6(b) shows the Von Mises stress σ_{VM} contours in N/cm² when $K_I \geq K_{Ic}$. The area around crack tip and the load point are enlarged in Fig. 6(b) to enable the clear view of contour.

The crack growth simulation is sufficiently carried out in four increment steps as shown in Fig. 7. As expected, the simulation clearly exhibits the pure mode I fracture path. Fig. 8 shows the experimental result for the compact tension specimen by [20].

4.2 Three Points Bend Specimen

The geometry of the three points bend specimen is illustrated in Fig. 9 where a is the crack length, W is the width and S is the span length. The analytical formula to calculate the stress intensity factor for the specimen is given by [18] as

$$K_I = \frac{6PS\sqrt{a}}{4BW^2} \frac{1.99 - \frac{a}{b} \left(1 - \frac{a}{b}\right) \left(2.15 - 3.93 \frac{a}{b} + 2.7 \left(\frac{a}{b}\right)^2\right)}{\left(1 + 2 \frac{a}{b}\right) \left(1 - \frac{a}{b}\right)^{3/2}} \quad (14)$$

where P is the applied load and B is the specimen thickness.

Consider the specimen as steel where the dimensions are $B = 1$ cm, $S = 32$ cm, $W = 8$ cm and $a = 4$ cm subjected to the applied load $P = 1$ KN. Under plane stress assumption, the calculated stress intensity factor is $K_I = 3.7652 \text{ MPa} \sqrt{\text{m}}$ with a relative error of 0.003 % compared to the analytical value which is $K_I = 3.7653 \text{ MPa} \sqrt{\text{m}}$.

Fig. 10 shows the final adaptive mesh, the normal principal stress and the Von Mises stress (MPa) for plane strain condition where $K_I > K_{Ic}$ and before performing the splitting node procedure.

The maximum value of σ_1 value was noticed at the crack tip. The maximum σ_{VM} value is at the constraint and loading points but the Von Mises stress σ_{VM} values at the crack tip is less than the yield stress. According to ASTM standard, in order to satisfy the plane strain condition, the specimen thickness must be $B \geq 2.5 \left(K_{Ic} / \sigma_Y\right)^2$ where σ_Y is the yield strength.

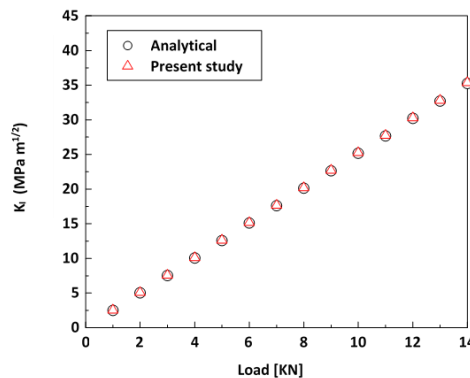


Fig. 5 Comparison of stress intensity factor, K_I values for aluminium specimen of thickness $B = 0.83$ cm

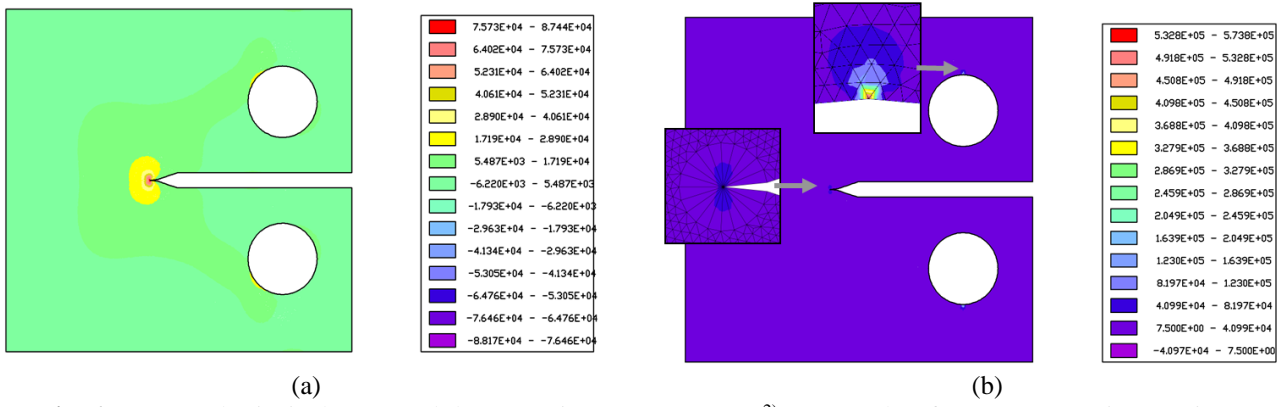


Fig. 6 (a) Normal principal stress and (b) Von Mises stresses (N/cm^2) contour plots for compact tension specimen.

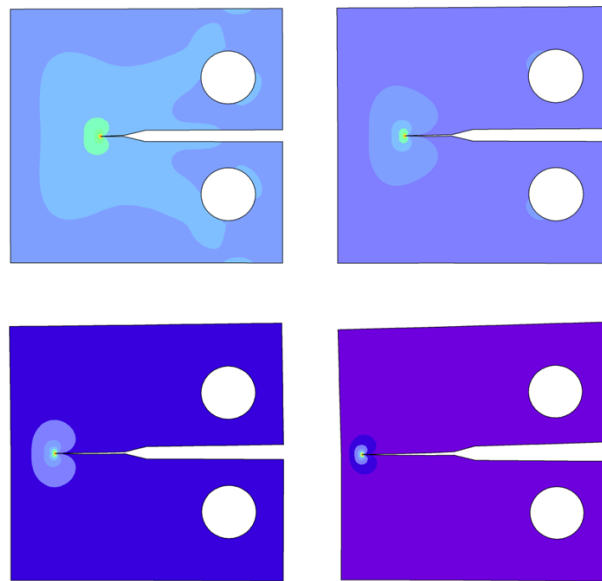


Fig. 7 Crack propagation simulation for the compact tension specimen

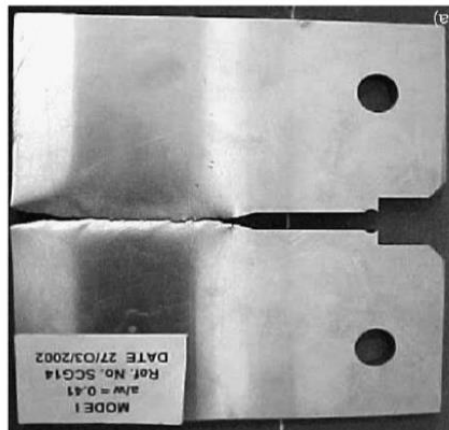


Fig. 8 Experimental crack trajectory for the compact tension specimen by [20]

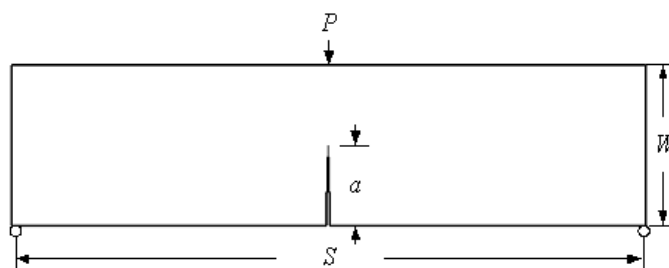


Fig. 9 Problem statement for the three points bend specimen

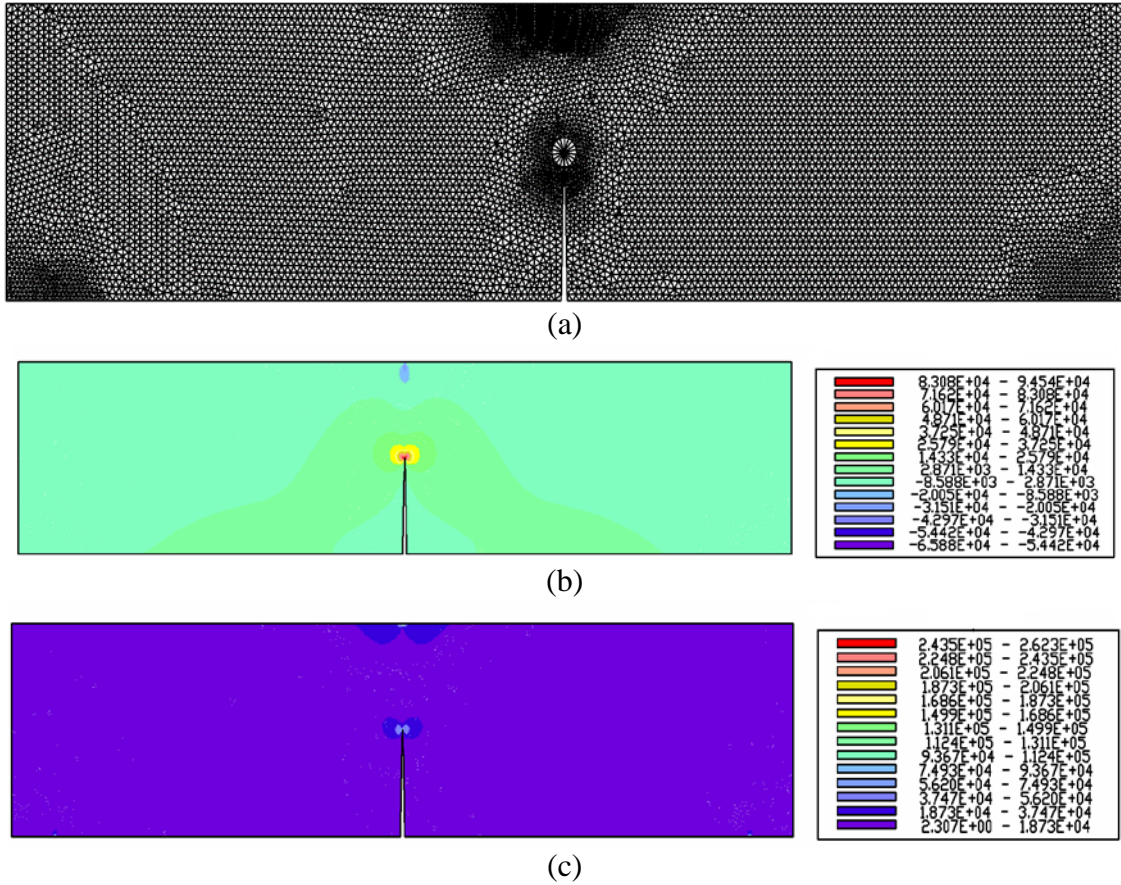


Fig. 10 (a) The adaptive mesh, (b) Normal principal stress and (c) Von Mises stress (10^{-2} MPa) contour plots for the three points bend specimen.

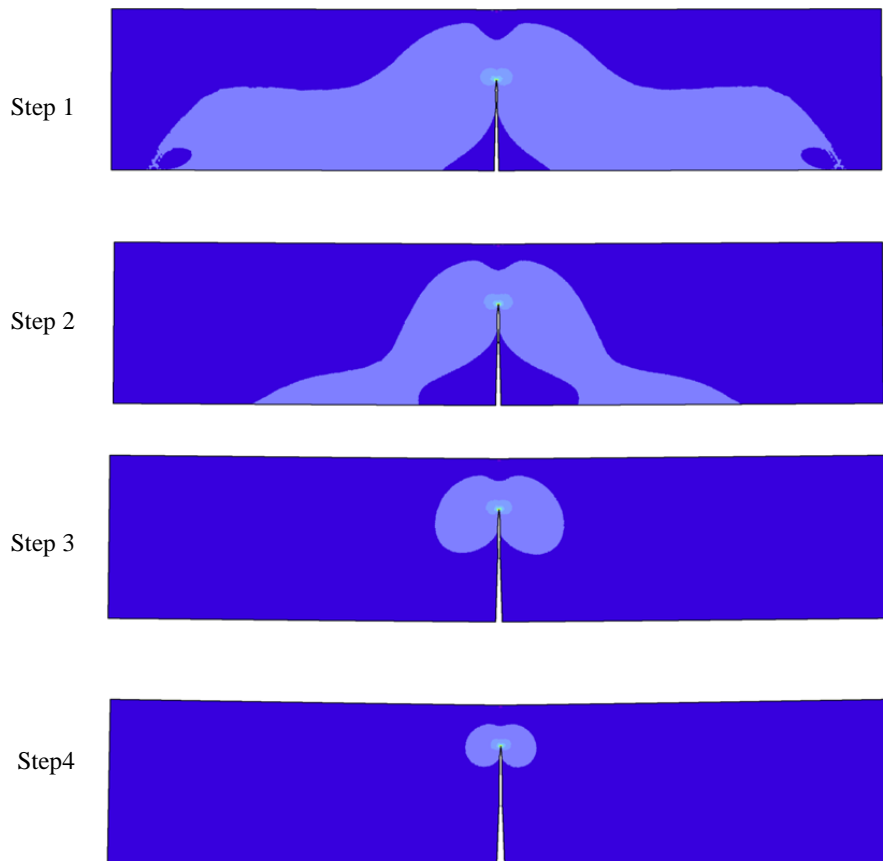


Fig. 11 Crack propagation simulation for the three points bend specimen

The crack propagation is shown in Fig. 11 in four crack increment steps. The crack path trajectory clearly follows the pure mode I fracture or pure opening mode which can be easily predicted from the boundary and loading conditions applied. The normal principal stress contour is plotted together merely to show the symmetrical pattern and the maximum value is always at the crack tip.

5. Conclusions

The simulation of crack propagation under linear elastic condition using dens mesh finite element method has been described in details. Furthermore, applying the global adaptive mesh refinement is essential in obtaining accurate stress intensity factor value, which a critical requirement in employing the displacement extrapolation technique. In addition, a dense rosette consisting of many singular elements is constructed around each of the crack tip to facilitate the calculation and also to correctly represent the stress field singularity in the vicinity of the crack tip. The fracture is modeled by the splitting node approach and the trajectory follows the successive linear extensions of each crack increment. The crack trajectories in the simulation qualitatively similar to the experimental and numerical results obtained by other researchers. This indicates that the developed program based on the dens mesh finite element method has been successfully predicted the crack growth direction and other related parameters.

References

- [1] J. A. George, *Computer implementation of the finite element method*, Ph.D Thesis, Computer Science Stanford University, USA, 1971.
- [2] S. Lo, A new mesh generation scheme for arbitrary planar domains, *International Journal for Numerical Methods in Engineering*, Vol. 21, No. 8, pp. 1403-1426, 1985.
- [3] J. Peraire, M. Vahdati, K. Morgan, O. C. Zienkiewicz, Adaptive remeshing for compressible flow computations, *Journal of computational physics*, Vol. 72, No. 2, pp. 449-466, 1987.
- [4] S. Lo, Dynamic grid for mesh generation by the advancing front method, *Computers & Structures*, Vol. 123, pp. 15-27, 2013.
- [5] M. Malekan, L. L. Silva, F. B. Barros, R. L. Pitangueira, S. S. Penna, Two-dimensional fracture modeling with the generalized/extended finite element method: An object-oriented programming approach, *Advances in Engineering Software*, Vol. 115, pp. 168-193, 2018.
- [6] Y. Liu, G. Glass, Choose the Best Element Size to Yield Accurate FEA Results While Reduce FE Models's Complexity, *British Journal of Engineering and Technology, Vols*, Vol. 1, pp. 13-28, 2013.
- [7] N. Benamara, A. Boulououar, M. Aminallah, N. Benseddiq, On the mixed-mode crack propagation in FGMs plates: Comparison of different criteria, *Structural Engineering and Mechanics*, Vol. 615, No. 3, pp. 371-379, 2017.
- [8] S. Soman, K. Murthy, P. Robi, A simple technique for estimation of mixed mode (I/II) stress intensity factors, *Journal of Mechanics of Materials and Structures*, Vol. 13, No. 2, pp. 141-154, 2018.
- [9] M. Yaylaci, The investigation crack problem through numerical analysis, *Structural Engineering and Mechanics*, Vol. 57, No. 6, pp. 1143-1156, 2016.
- [10] S. P. Jena, D. R. Parhi, D. Mishra, Comparative study on cracked beam with different types of cracks carrying moving mass, *Structural Engineering and Mechanics*, Vol. 56, No. 5, pp. 797-811, 2015.
- [11] S. T. More, R. Bindu, Effect of mesh size on finite element analysis of plate structure, *Int. J. Eng. Sci. Innovative Technol*, Vol. 4, No. 3, pp. 181-185, 2015.
- [12] A. M. Alshoaibi, Finite element procedures for the numerical simulation of fatigue crack propagation under mixed mode loading, *Structural Engineering and Mechanics*, Vol. 35, No. 3, pp. 283-299, 2010.
- [13] A. M. Alshoaibi, An Adaptive Finite Element Framework for Fatigue Crack Propagation under Constant Amplitude Loading, *International Journal of Applied Science and Engineering*, Vol. 13, No. 3, pp. 261-270, 2015.
- [14] R. S. Barsoum, Application of quadratic isoparametric finite elements in linear fracture mechanics, *International Journal of Fracture*, Vol. 10, No. 4, pp. 603-605, 1974.
- [15] R. Henshell, K. Shaw, Crack tip finite elements are unnecessary, *International journal for numerical methods in engineering*, Vol. 9, No. 3, pp. 495-507, 1975.
- [16] G. V. Guinea, J. Planas, M. Elices, KI evaluation by the displacement extrapolation technique, *Engineering fracture mechanics*, Vol. 66, No. 3, pp. 243-255, 2000.
- [17] F. Erdogan, G. Sih, On the crack extension in plates under plane loading and transverse shear, *Journal of basic engineering*, Vol. 85, No. 4, pp. 519-525, 1963.
- [18] J. E. Srawley, Wide range stress intensity factor expressions for ASTM E 399 standard fracture toughness specimens, *International Journal of Fracture*, Vol. 12, No. 3, pp. 475-476, 1976.
- [19] L. Parnas, Ö. G. Bilir, E. Tezcan, Strain gage methods for measurement of opening mode stress intensity factor, *Engineering fracture mechanics*, Vol. 55, No. 3, pp. 485-492, 1996.
- [20] A. Mourad, M. Alghafri, O. A. Zeid, S. Maiti, Experimental investigation on ductile stable crack growth emanating from wire-cut notch in AISI 4340 steel, *Nuclear engineering and design*, Vol. 235, No. 6, pp. 637-647, 2005.